Pramana – J. Phys. (2020) 94:97
https://doi.org/10.1007/s12043-020-01972-3

Evaluation of the gamma and neutron shielding properties of $64TeO_2 + 15ZnO + (20 - x)CdO + xBaO + 1V_2O_5$ glass system using Geant4 simulation and Phy-X database software

A AŞKIN

Department of Electrical and Electronics Engineering, Munzur University, Tunceli, Turkey
E-mail: aliaskin@munzur.edu.tr

MS received 20 October 2019; revised 3 February 2020; accepted 22 April 2020

Abstract. In this study, fast neutron removal cross-section and γ-ray shielding capabilities in terms of mass attenuation coefficient (μ_m), transmission fractions (T), effective atomic numbers (Z_{eff}), half-value layer (HVL) and exposure build-up factors (EBF) of the $64TeO_2 + 15ZnO + (20 - x)CdO + xBaO + 1V_2O_5$ ($x = 0, 5, 10, 15, 20$ mol%) glass system have been evaluated using Monte Carlo simulations carried out with Geant4 model of the high-purity germanium (HPGe) detector and Phy-X database software. The results of this study revealed that γ-ray shielding capability of the studied glass system increases with the increase of BaO content and decrease of CdO content in the chemical structure due to the high atomic number (Z) of Ba compared to Cd. The results also showed that increase of BaO fraction in the glass structure weakens the neutron shielding ability and by the use of low Z elements in the composites better shielding performance against neutrons can be obtained.

Keywords. Photon attenuation; glasses; fast neutron removal; Geant4; Phy-X.

PACS Nos 07.05.Tp; 29.30.Kv; 29.40.Wk

1. Introduction

Radioactive isotopes are actively used in various fields of technology including health care, aerospace, nuclear powerplants, research and accelerator centres. Therefore, materials used in areas where radiation exposure is possible, must have good gamma and neutron shielding abilities to decrease the intensity of incident radiation to an acceptable level to protect the health of individuals against the possible hazardous effects of gamma and neutron radiations. Many researchers have investigated and reported the shielding properties of various natural materials. Gamma-ray shielding properties of granite, andesite, basalt and tuff stones mined from different cities in Turkey have been computationally investigated using the Monte Carlo simulations [1]. Gamma blocking abilities of two different clay materials from Nigeria were investigated experimentally by using high-purity germanium detector (HPGe) [2]. Linear and mass attenuation coefficients of different types of sand, soil and beach mineral samples were evaluated in the energy range between 276 and 1332 keV [3]. Photon shielding abilities of some fatty acids were calculated experimentally using NaI(Tl) detector [4]. Not only naturally occurring materials but also synthetically developed and produced composite materials have been assessed in terms of their radiation shielding capabilities. Shielding capabilities of heavyweight concrete were determined experimentally by Gokce *et al* [5]. Gamma-ray attenuation characteristics of the Zn–Cd–Sn–Pb alloys were determined at 511 and 662 keV photon energies by Kaur *et al* [6]. Monte Carlo simulations were carried out to evaluate the radiation shielding capabilities of different steel alloys [7]. Photon shielding parameters of gadolinium-containing polymeric compounds were computationally determined from the Monte Carlo simulations performed with the Geant4 and MCNPX simulation toolkits [8].

Optical properties and transparency to visible light, easy preparation and production, good neutron and gamma absorbtion properties of glasses make them attractive to researchers and tremendous work is going on to develop glasses doped with different types of elements or compounds to improve their optical, physical,

Published online: 02 July 2020

thermal and radiation shielding capabilities. Radiation shielding characteristics of six different PbO–Li_2O–B_2O_3 glass samples were experimentally determined at four different γ-ray energies by Kumar [9]. Photon attenuation properties of the lanthanum calcium silicoborate glasses and the effect of La_2O_3 on the attenuation properties were experimentally evaluated at eight different photon energies between 224 keV and 662 keV [10]. Gamma and neutron attenuation properties of BaO/SrO–Bi_2O_3–B_2O_3 glasses were determined computationally via Monte Carlo simulations using the MCNP5 toolkit and WinXCom database software [11].

Tellurite glasses have good non-linear optical properties, chemical resistance, good dielectric properties and good solubility of heavy metal ions [12]. Previous researches also revealed that the silicate-based [13], Bi_2O_3-based [14] and the tellurite-based glasses [15] have very good shielding abilities.

$64TeO_2 + 15ZnO + (20 - x)CdO + xBaO + 1V_2O_5$ ($x = 0, 5, 10, 15, 20$ mol%) glass system were prepared and its structural, thermal and optical properties were investigated by Sreenivasulu *et al* [16]. In this study, mass attenuation coefficient (μ/ρ), transmission fraction, half value layer (HVL) , effective atomic number (Z_{eff}), effective electron density (N_{eff}), exposure build-up factor (EBF) and fast neutron removal cross-section parameters of this glass system were computationally investigated using Monte Carlo simulations performed with the Geant4 model of an HPGe detector and the Phy-X database software.

2. Materials and methods

2.1 *Theoretical background*

Beer–Lambert's law given in eq. (1) is the widely used formula to calculate the attenuation amount of the γ-ray photons travelling through a medium.

$$I = I_0 \cdot e^{-\mu \cdot x}, \tag{1}$$

where I_0 and I are the incident and attenuated photon intensities respectively, x (cm) is the thickness of the material and μ (cm^{-1}) is the linear attenuation coefficient of the sample. For each studied gamma energy, I_0 can be determined without the sample placed between the γ-ray source and the detector. Determination of the parameter I relies on the existence of sample between the source and the detector and for each new sample thickness, this parameter must be determined separately. The value of $\ln(I_0/I)$ vs. the thickness of the sample is plotted. The slope of the linear fit to these data gives μ at the studied photon energy.

The mass attenuation coefficient, μ_m ($cm^2 \cdot g^{-1}$), is the interaction probability of the γ-ray photons within a material and it is calculated by using eq. (2).

$$\mu_m = \mu/\rho, \tag{2}$$

where ρ is the density ($g \cdot cm^{-3}$) of the absorbing material.

The ratio of the transmitted photon intensity (I) to the incident photon intensity (I_0) results in the transmission fraction (T) of the γ-ray photons through the materials. This parameter provides an important information about the gamma blocking ability of a material and can be calculated using eq. (3).

$$T = I/I_0. \tag{3}$$

Thickness at which the intensity of the incident radiation reduces by one-half is defined as the half-value layer (HVL) and it can be calculated by using the linear attenuation coefficient (μ) as given in eq. (4).

$$\text{HVL} = \ln(2)/\mu. \tag{4}$$

Composite materials are characterised by a number known as effective atomic number (Z_{eff}) and it provides conclusive information for materials. This parameter can be calculated by using the following equation [17]:

$$Z_{\text{eff}} = N_{\text{A}} \frac{\sum_i f_i A_i (\mu/\rho)_i}{\sum_j f_j A_j / Z_j (\mu/\rho)_j}, \tag{5}$$

where N_{A} is the Avogadro's number, A_i and A_j are the atomic weights, f_i and f_j are the numbers of atoms and Z_i, Z_j represent the atomic numbers of the ith and jth elements respectively.

The exposure build-up factors (EBF) of any material can be calculated using equivalent atomic number (Z_{eq}) and G-P fitting parameters. As the interaction processes of γ-rays within any material depend on the energy of γ-ray, Z_{eq} varies according to the energy of the interacting γ-rays. Thanks to the use of this parameter, a composite material can be described similar to a single element with atomic number Z. This parameter can be calculated using eq. (6) [20].

$$Z_{\text{eq}} = \frac{(\mu/\rho)_{\text{Compton}}}{(\mu/\rho)_{\text{total}}}. \tag{6}$$

The G-P parameters of a, b, c, d and X_k for elements are taken from the database report of the American Nuclear Society (ANSI/ANS-6.4.3) and they were utilised to calculate the EBF parameters from the G-P fitting formula given in eqs (7)–(9) [21].

$$B(E, X) = 1 + \frac{b-1}{K-1}(K^X - 1) \quad \text{for } K \neq 1, \tag{7}$$

$$B(E, X) = 1 + (b-1)X \quad \text{for } K = 1, \tag{8}$$

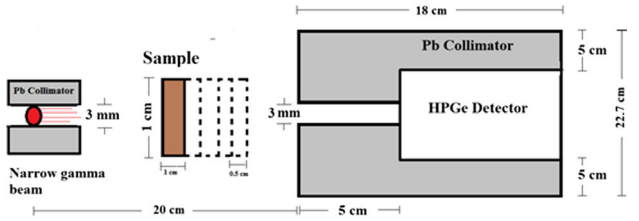

Figure 1. Schematic of the Geant4 set-up.

$$K(E, X) = cX^a + d\frac{\tanh(X/X_k - 2) - \tanh(-2)}{1 - \tanh(-2)}, \quad (9)$$

where E is the incident photon energy and X is the penetration depth (in mean free path, mfp).

Fast neutron removal cross-section or neutron attenuation coefficient (Σ_R, cm^{-1}) is a measure of the likelihood that a penetrating fast neutron undergoes a first collision which removes it from the group of uncollided neutrons [18]. As fast neutrons are not directly absorbed during their passage through the material, they will first slow down by the elastic collisions with the nuclei of light elements. When their energy is reduced to the thermal energy (0.025 eV), they are absorbed by the nuclei of heavy elements by means of the radiative capture [19]. As the glass specimens investigated in the present study contain both light and heavy elements, investigation of their neutron shielding capabilities will provide information about their applicability in the fast neutron-containing areas. Similar to γ-ray attenuation coefficients, Σ_R, cm^{-1} for composites or homogeneous mixtures can be calculated using eqs (10) and (11) [18].

$$\frac{\Sigma_R}{\rho} = \sum_i W_i \left(\frac{\Sigma_R}{\rho}\right)_i, \quad (10)$$

$$\Sigma_R = \sum_i \rho_i \left(\frac{\Sigma_R}{\rho}\right)_i, \quad (11)$$

where W_i represents the weight fraction of each element in the chemical composition.

2.2 *Monte Carlo simulations*

Mass attenuation coefficient (MAC) values of the selected glass system have been evaluated using the Geant4 model of an HPGe detector. The entire geometry and structure of the detector were coded into Geant4 to perform the Monte Carlo simulations. The details of the used Geant4 model is given in [1]. As shown in figure 1, the detector and the γ-ray source were housed in a lead shield with a hole of 3 mm diameter created at centres of both shields to create narrow-beam γ-rays to validate the Beer–Lambert's law. The chemical structure and the densities of the materials coded as TZCB1,

Table 1. Chemical composition parameters of the $64TeO_2 + 15ZnO + (20 - x)CdO + xBaO + 1V_2O_5$ glass system.

Glass sample	Glass structure	Density (g/cm^3)	Mass fraction of elements (%)					
			Te	O	Zn	Cd	Ba	V
TZCB1	$64TeO_2$+15ZnO+20CdO +0BaO+$1V_2O_5$	5.670	57.57	18.95	6.91	15.85	0.0	0.72
TZCB2	$64TeO_2$+15ZnO+15CdO +5BaO+$1V_2O_5$	5.604	57.07	18.78	6.85	11.78	4.800	0.71
TZCB3	$64TeO_2$+15ZnO+10CdO +10BaO+$1V_2O_5$	5.527	56.58	18.62	6.80	7.79	9.51	0.71
TZCB4	$64TeO_2$+15ZnO+5CdO +15BaO+$1V_2O_5$	5.476	56.09	18.46	6.74	3.86	14.15	0.70
TZCB5	$64TeO_2$+15ZnO+0CdO +20BaO+$1V_2O_5$	5.390	55.62	18.31	6.68	0.0	18.70	0.69

Table 2. Mass attenuation coefficients of the TZCB glass system calculated using Geant4 and Phy-X software.

Glass sample	0.284 MeV		0.347 MeV		0.511 MeV		0.662 MeV		0.826 MeV		1.17MeV		1.33 MeV	
	Geant4	Phy-X	Geant4	Phy-X	Geant4	Phy-X	Geant4	Phy-X	Geant4	Phy-X	Geant4	Phy-X	Geant4	Phy-X
TZCB1	0.156	0.162	0.124	0.127	0.092	0.090	0.077	0.075	0.060	0.065	0.049	0.053	0.047	0.050
TZCB2	0.159	0.164	0.125	0.128	0.093	0.090	0.078	0.075	0.063	0.065	0.050	0.053	0.047	0.050
TZCB3	0.163	0.166	0.128	0.129	0.096	0.090	0.080	0.075	0.064	0.065	0.052	0.053	0.048	0.050
TZCB4	0.166	0.167	0.131	0.130	0.097	0.091	0.081	0.075	0.067	0.066	0.055	0.053	0.049	0.050
TZCB5	0.170	0.169	0.135	0.131	0.099	0.091	0.083	0.076	0.070	0.066	0.056	0.053	0.050	0.050

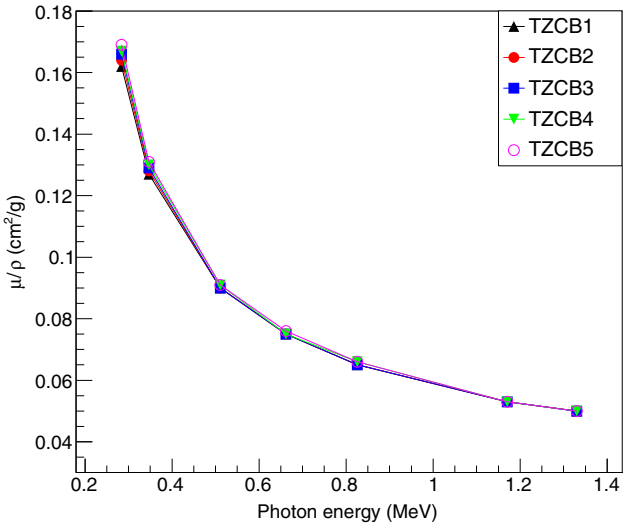

Figure 2. Change of mass attenuation coefficients (μ/ρ) with respect to photon energy.

2, 3, 4 and 5 are given in table 1 [16]. Weight fractions and the densities were used as inputs into Geant4 to define the structure of glasses for the simulations. Monte Carlo simulations were performed at photon energies of 0.284 MeV (^{137}Cs), 0.347 MeV (^{60}Co), 0.511 MeV (^{22}Na), 0.662 MeV (^{137}Cs), 0.826 MeV (^{60}Co), 1.173 MeV (^{60}Co) and 1.330 MeV (^{60}Co). For each studied energy, the simulations were first run without placing the glass samples between the source and the detector to obtain the incident photon intensity (I_0). Then, the simulations were run with the glass sample between the source and the detector. For each energy, simulations were carried out for the glass samples of 1 cm, 1.5 cm, 2 cm, 2.5 cm and 3 cm thickness to evaluate the amount of attenuated photon intensity (I) for each thickness.

2.3 *Phy-X software*

Phy-X software is a newly developed tool for calculating diverse shielding parameters including linear and mass attenuation coefficients, half value and tenth value layer, mean free path, effective atomic number and electron densities, energy absorption and build-up factors in the energy region between 1 keV and 100 GeV [22]. The calculation of each aforementioned parameter is done by the software using chemical composition entered either in mole or weight fraction and the density of the material.

3. Results and discussion

MAC values of the $64TeO_2$+$15ZnO$ +$(20-x)CdO$+ $xBaO$+$1V_2O_5$ glass system were calculated using Geant4 Monte Carlo simulations and Phy-X software.

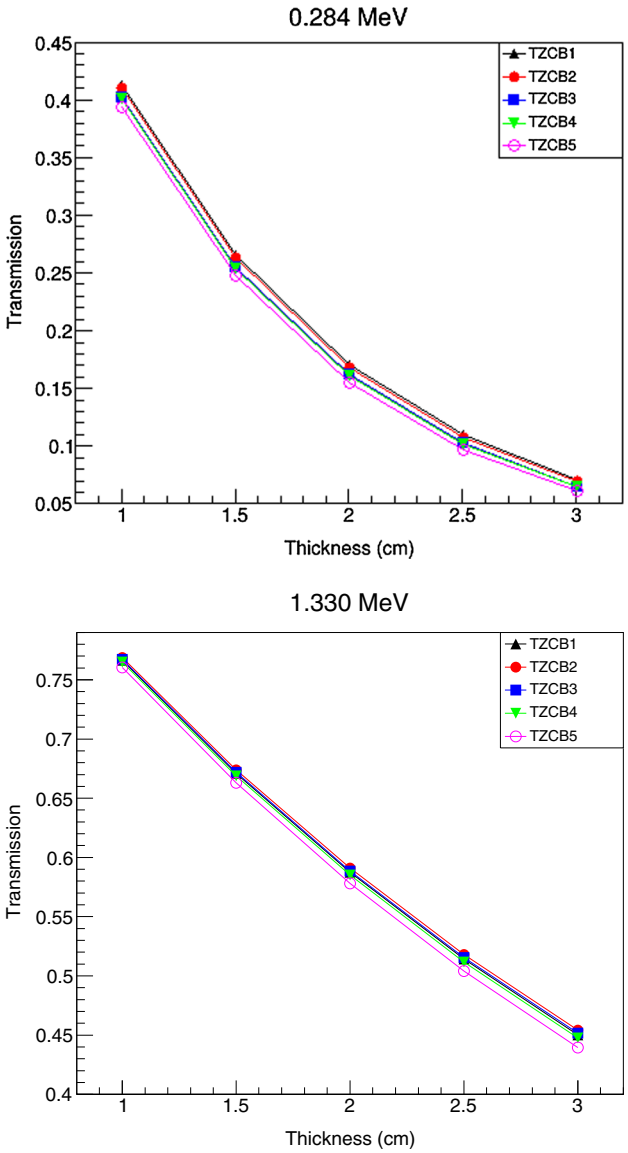

Figure 3. Transmission factor vs. thickness of TZCB glass system at 0.284 and 1.33 MeV photon energies.

The results from both toolkits are given in table 2. The relative difference (RD) between the results were calculated using eq. (12).

$$\mathrm{RD} = \frac{R_G - R_P}{R_G} \times 100, \tag{12}$$

where R_G and R_P are the mass attenuation coefficients from the Geant4 and Phy-X respectively.

The mean and standard deviations of the calculated RD values were used to benchmark the agreement between the results obtained using the two different toolkits. Mean and standard deviations of the RD values were found to be (3.9±2.2)%. As the attained RD is around 6% [23], it can be concluded that the results from both toolkits are in agreement and reliable. The trend of

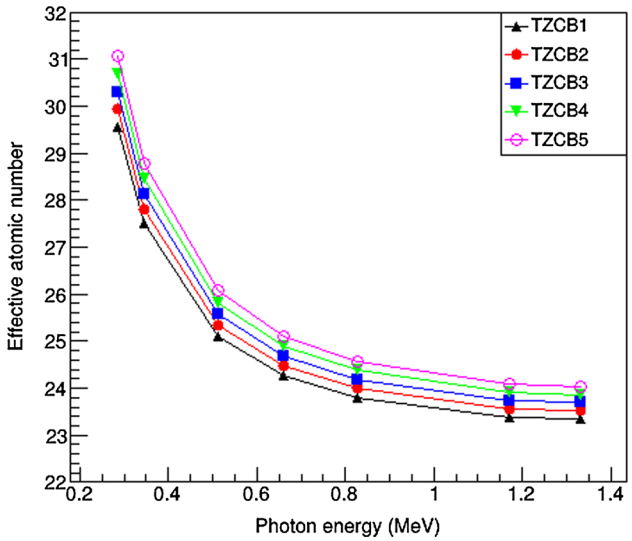

Figure 4. Variation of the effective atomic number (Z_{eff}) with respect to photon energy.

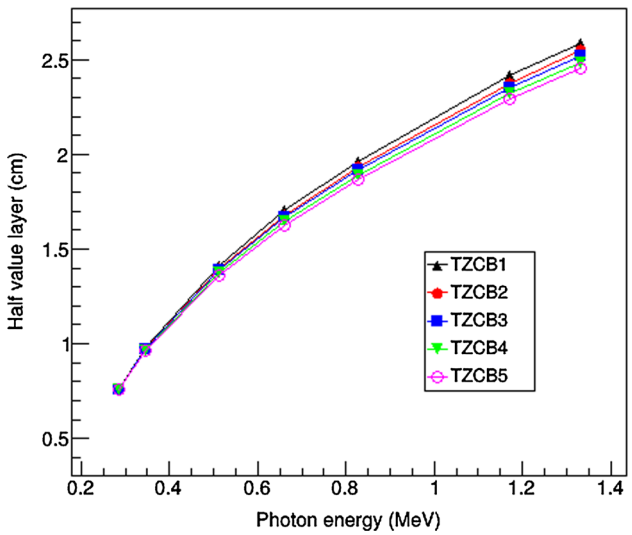

Figure 5. Half value layer of the TZCB glass systems as a function of photon energy.

MAC is visualised in figure 2. At the low energy sides, the MAC values are high and decrease sharply till 1.100 MeV. After that, the change in the values are slight and they remain almost constant. This is due to the interaction processes of the γ-rays within the materials. At low energy sides the photoelectric process dominates and this process strongly depends on the chemical structure and the atomic number (Z) of the materials. At high energy sides (above 1.100 MeV), pair production is the dominating interaction process and dependence on Z is weak.

Transmission fraction (T) is an important parameter showing the gamma blocking ability of the materials.

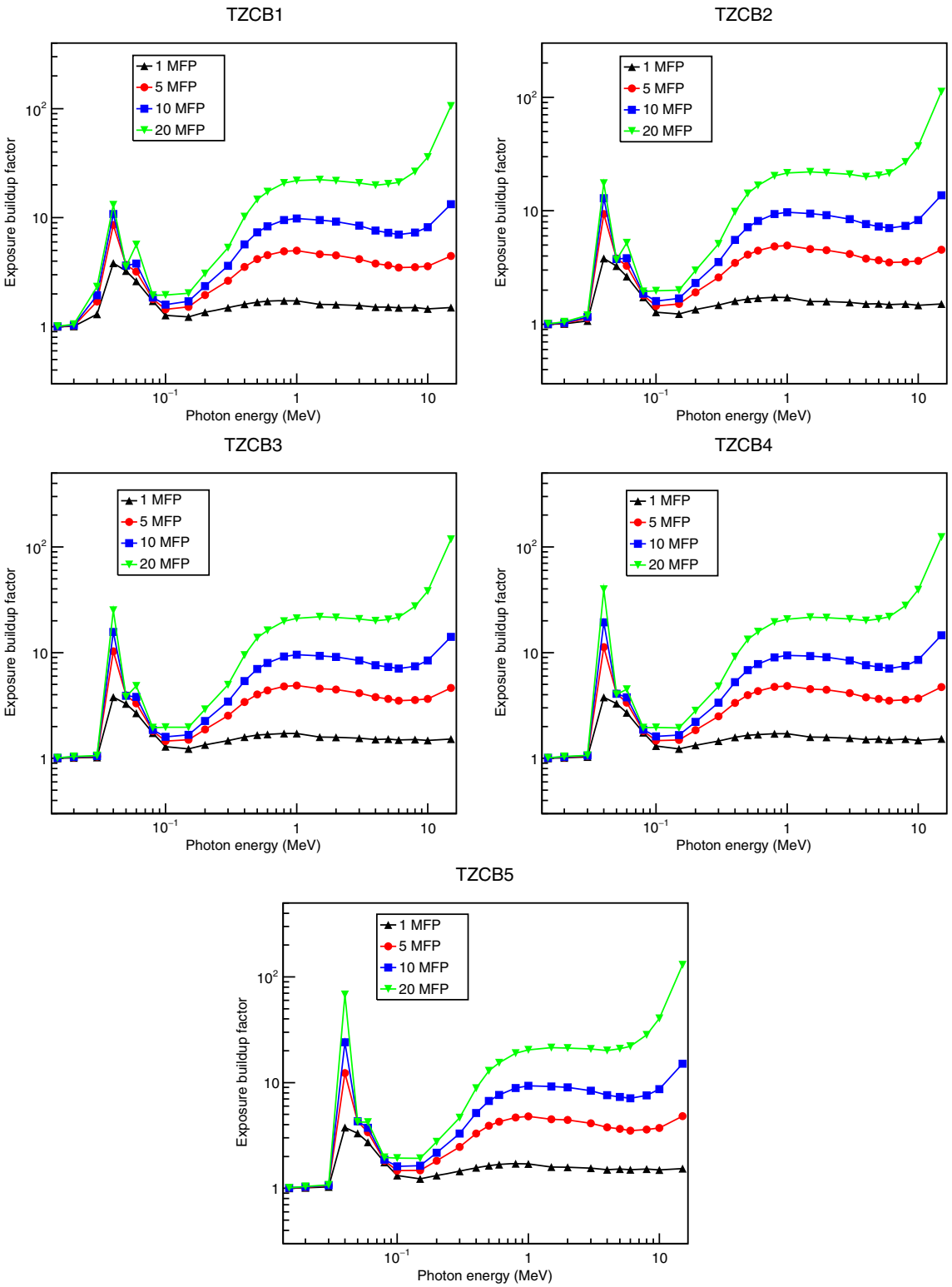

Figure 6. Variation of EBF with photon energy for the penetration depth of 1, 5, 10 and 20 mfp.

Thanks to the use of materials with low T values, better shielding performance can be obtained by using thin layer of materials. Figure 3 shows the dependence of the transmission of γ-ray photons on the thickness of the glass system at 0.284 and 1.330 MeV. As can be seen from these plots, TZCB5 glass has low T values compared to TZCB1. High amount of BaO in the TZCB5 structure results in a low transmission due to the high atomic number of Ba ($Z = 56$) compared to Cd ($Z = 48$). High-energy γ-rays have more penetration and diffusion abilities. Figure 3 also reveals that thick glass samples are needed to attenuate the intensity of the high-energy γ-rays to an acceptable level.

The dependence of Z_{eff} of the studied glass system on the energy of incoming photons is shown in figure 4. The Z_{eff} values of all TZCB glass system are different from each other. With the increase of the mass fraction of BaO and the decrease of the mass fraction of CdO, the effective atomic number of the glass system is found to be increasing which is obvious too because atomic number of Ba is higher than that of Cd. This increase in Z_{eff} with increase of Ba amount suggests that the shielding ability of glasses increases with the addition of BaO. Among the glasses studied in the present work, TZCB5 and TZCB1 possess the highest and the lowest values of Z_{eff} respectively at the photon energies between 0.284 and 1.33 MeV. It is observed that Z_{eff} initially decreases sharply till 662 keV. The decrease becomes slower between 662 and 1100 keV and Z_{eff} tends to remain stable on the higher side of γ-ray energy due to the dominance of incoherent (Compton) scattering and pair production processes.

The HVL is a significant parameter characterising the shielding capability of the materials. Thanks to the use of materials with low HVL values, better shielding performances can be achieved by the use of thin layers. In figure 5, HVL values of the TZCB glass system are plotted with respect to the photon energies. As can be seen in this plot, TZCB5 glass has the lowest and TZCB1 has the highest values of HVL at the given photon energies. Depending on the photon energy, increasing BaO concentration from 0 to 20% moles, causes a decrease in the HVL due to the high atomic number of Ba.

The exposure build-up factors (EBF) of the TZCB glass system has been calculated for the γ-ray energies between 15 keV and 15 MeV and for the penetration depths of 1, 5, 10 and 20 mfp (mean free path). Figure 6 shows the change in EBF values with respect to the photon energy. As these plots revealed, increasing BaO fraction from 0 to 20% moles and decreasing the CdO content from 20 to 0% moles does not significantly effect the values of EBF above 0.1 MeV. The EBF parameters have small values in low-energy region because the low-energy γ-rays are completely absorbed due to the photoelectric process. For photon energies above 0.1 MeV, the EBF values tend to increase due to the dominating Compton scattering process. For all TZCB glass samples, EBF has small values for 1 mfp penetration depth and EBF increases due to the multiple scattering events occurring in higher penetration depths. For TZCB1 glass, the sharp peak observed at around 0.03 MeV is due to the k edge absorbtion of Te (0.032 MeV) and this peak increases as the fraction of BaO in the composition increases. Depending on the BaO fraction, the k edge absorbtion of Ba at 0.037 keV cause gradual increase in the intensity of the peak.

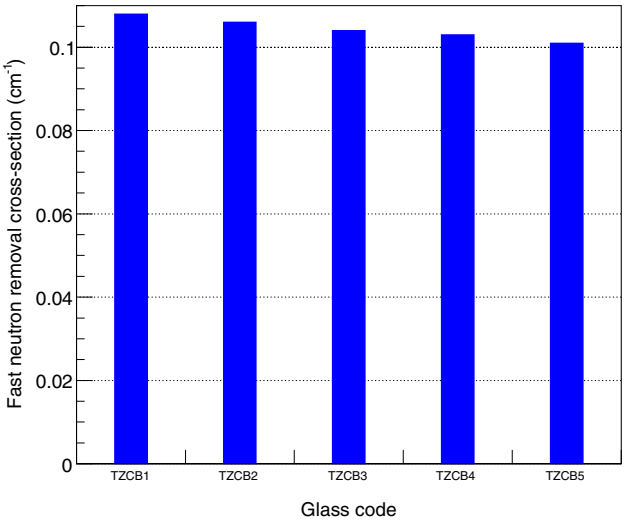

Figure 7. Fast neutron removal cross-section of TZCB glasses.

The removal cross-section for the fast neutrons is shown in figure 7. As can be seen clearly in this plot, the removal cross-section is 0.109 for the TZCB1 glass which gradually decreases to 0.101 for the TZCB5 glass. Low atomic number of Cd compared to Ba results in a better shielding performance against the fast neutrons.

4. Conclusion

In this study, gamma and neutron shielding characteristics of the TeO_2+ZnO+CdO+BaO+V_2O_5 (TZCB) glass system were evaluated computationally from the Monte Carlo simulations carried out using Geant4 simulation toolkit and Phy-X database software. The results showed that the mass attenuation values calculated using the two different toolkits are in agreement. The results of the present study also revealed that the increase in the BaO content and the same amount of decrease in the CdO content of the TZCB glass system increases the mass attenuation coefficient and effective atomic number, therefore, decreases the transmission fraction and

HVL. Increase of BaO improves the shielding capability due to the high atomic number of Ba compared to Cd. The results of this study also showed that low Z materials, used even in compounds, enhance the neutron blocking ability and TZCB1 glass with 0% moles of BaO has higher removal cross-section than TZCB5 glass with 20% moles of BaO existed in its structure.

Acknowledgements

The author would like to express his gratitude to the editor(s) and reviewer(s) for their valuable and constructive comments.

References

[1] A Askin, *Pramana – J. Phys.* **93**: 14 (2019)
[2] S F Olukotun, S T Gbenu, F I Ibitoye, O F Oladejo and H O Shittu, *Nucl. Eng. Technol.* **50**(**6**), 957 (2018)
[3] M N Alam, M M Miah, M I Chowdhury, M Kamal and S Ghose, *Appl. Radiat. Isot.* **54**, 973 (2001)
[4] D K Gaikwad, P P Pawar and T P Selvam, *Pramana – J. Phys.* **87**: 12 (2016)
[5] H S Gokce, B C Ozturk, N F Cam and O A Cakir, *Cement Concrete Comp.* **92**, 56 (2018)
[6] T Kaur, J Sharma and T Singh, *Radiat. Phys. Chem.* **156**, 90 (2019)
[7] V P Singh, M E Medhat and S P Shirmardi, *Radiat. Phys. Chem.* **106**, 255 (2015)
[8] F Tabbakh, *Pramana – J. Phys.* **86**, 939 (2016)
[9] A Kumar, *Radiat. Phys. Chem.* **136**, 50 (2017)
[10] S Kaewjaeng, S Kothan, N Chanthima, H Kim and J Kaewkhao, *Mater. Today Proc.* **5**, 14901 (2018)
[11] M I Sayyed, G Lakshminarayana, M G Dong, M C Ersundu and A E Ersundu, *Radiat. Phys. Chem.* **145**, 26 (2018)
[12] R El-Malawany, *J. Appl. Phys.* **72**, 1774 (1992)
[13] K Kirdsiri, J Kaewkhao, N Chathima and P Limsuwan, *Ann. Nucl. Energy* **38**, 1438 (2011)
[14] M G Dong *et al. J. Non-Cryst. Solids* **468**, 12 (2017)
[15] M I Sayyed, S I Qashou and Z Y Khattari, *J. Alloys Compd.* **696**, 632 (2017)
[16] V Sreenivasulu, G Upender, V C Mouli and M Prasad, *Spectrochim. Acta A* **148**, 2015 (2015)
[17] S R Manohara, S M Hanagodimath and L Gerward, *J. Nucl. Mater.* **393**, 465 (2009)
[18] M F Kaplan, *Concrete radiation shielding* (John Wiley & Sons Inc, New York, 1989)
[19] A B Chilton, J K Shultis and R E Faw, *Principles of radiation shielding* (Prentice-Hall, New York, 1984)
[20] V P Singh, N M Badiger, N Chanthima and J Kaewkhao, *Radiat. Phys. Chem.* **98**, 14 (2014)
[21] Y Harima, *Radiat. Phys. Chem.* **41**, 631 (1993)
[22] E Sakar, O F Ozpolat, B Alim, M I Sayyed and M Kurudirek, *Radiat. Phys. Chem.* **166**, 108496 (2020)
[23] O Agar, M I Sayyed, F Akman, H O Tekin and M R Kacal, *Nucl. Eng. Technol.* **52**, 853 (2019)